PHYSICAL REVIEW B VOLUME 17, NUMBER 12 15 JUNE 1978

Uniaxially stressed silicon: Fine structure of the exciton and deformation potentials

J.-C. Merle,* M. Capizzi, and P. Fiorini
Istituto di Fisica, Università di Roma, Roma, Italy

A. Frova
Istituto di Fisica, Università di Modena, Modena, Italy

(Received 17 January 1978)

The splitting of the indirect exciton in Si is measured, at the TO-phonon-assisted threshold, as a zero-stress extrapolation of the multiplet structure due to uniaxial stresses applied in the [001] direction. The validity of the method is warranted by a theoretical analysis of the exciton wave functions and energy levels under the combined influence of mass anisotropy and external perturbation. For the splitting, a value of 0.29 ± 0.05 meV is found and compared with the latest theoretical estimate of the mass-anisotropy effect which includes coupling with the split-off valence band; the measured splitting, however, may include a contribution from exchange interaction. The intensities of the exciton components for moderately high stress are quite consistent with those calculated for an indirect transition mechanism involving only two intermediate states Γ_{15} and Δ_5 which can produce interference. In the limit of zero stress, a ratio of the intensities of the doublet components $\eta = 5.7 \pm 0.5$ is determined. The experiment allows also a direct measurement of the deformation potentials, giving results in very good agreement with pseudopotential calculations.

I. INTRODUCTION

The interest in the investigation of fine spectral structures of the exciton in semiconductors and in the determination of its basic parameters (effective Rydberg, excited states, splitting, intrinsic broadening) has been mainly promoted by the recent development of the physics of electron-hole systems at high densities. On the other hand, theoretical analyses in terms of the effective-mass approximation have now become available. Their verification by a thorough experimental characterization of the exciton can justify, for instance, the validity of the static screening assumption and elucidate the role of the Coulomb part in the more general context of impurity problems. Experimentally, current-modulation techniques do allow standards of resolution which are adequate on a $\frac{1}{10}$-meV scale, characteristic of excitonic splittings in indirect-gap semiconductors.

The main origin of the exciton splitting, in absence of external perturbations, is the degeneracy of the hole, combined with the mass anisotropy of the electron which prevents the negative charge from being spherically distributed around the hole. Exchange effects may also play a role, although they are generally believed to be of minor importance in indirect semiconductors. We shall hereafter call Δ' the overall splitting, as observed experimentally, and Δ the part due to the mass anisotropy alone. The materials which have received so far the most attention are germanium, silicon, and gallium phosphide. The situation in germanium is fairly well established.[1] For GaP, which presents the anomaly of a camelback structure at the bottom of the conduction band, both theoretical[2] and experimental[3] investigations are at a stage of preliminary reports. In the present paper we intend to concentrate on silicon, a material where, despite extensive investigations, the results are still a matter of controversy.

As opposed to Ge and GaP, in silicon the 1S exciton state gives rise to a single, relatively broad, absorption band, exhibiting no resolved structure even in wavelength-modulation experiments.[4-7] A twofold splitting Δ' with level separation of 0.35 ± 0.05 meV and strength ratio $\eta = 3$ has been proposed by Balslev[7] after a double deconvolution procedure of the unresolved band. His method, however, is questionable on various aspects and we feel that the figure given for the interval of uncertainty is much too optimistic. Also recently, Thewalt and Parsons[8] have presented some direct evidence of a splitting, which they put at 0.20 ± 0.05 meV, although from their spectra for the strong TO-assisted excitonic transition we would rather argue in favor of a larger Δ', i.e., not less than 0.30 meV.

The above λ-modulation experiments were prompted by the work of Hammond *et al.*,[9] the first to give evidence—although indirect—of a level multiplicity. In the range 2–10 K, they observed a temperature dependence in the relative strengths of the TO-phonon-assisted and LO-phonon-assisted free-exciton luminescence. A model in terms of a pair of transitions, with phonon-dependent selection rules, proved quite satisfactory in explaining the experimental behavior. The splitting Δ' was

used as a best-fitting parameter. According to their latest publication,[10] they find $\Delta' = 0.4 \pm 0.1$ meV. In the treatment, the exciton system was assumed to be in thermal equilibrium with the lattice. A higher exciton effective temperature might have reduced the value of the splitting.

On the theoretical side, exchange effects are generally neglected, while for the mass-anisotropy splitting there is a widespread of results of chronologically increasing reliability. The problem is discussed at length in Ref. 11. A perturbation approach[12] yields $\Delta = 0.30$ meV, but the agreement with the experimental data mentioned above is likely to be fortuitous, as the variational method later used by Lipari and Altarelli,[11] which gives in germanium results in perfect agreement with the observation,[13] for equal material parameters leads to $\Delta = 0.46$ meV. The difference in silicon is that the spin-orbit split-off valence band is much closer to the upper degenerate band than in germanium. None of the above theoretical approaches takes this into account. A preliminary calculation by Lipari and Altarelli[14] shows that interaction with the split-off valence band lowers the splitting to 0.32 meV. This is probably the most accurate value to date.

The general situation in silicon is summarized in Table I, where we also give an anticipation of the data to be found in the present experiment, which will be discussed in the closing part of the paper.

Scope of this work is to draw conclusive results as to the value of the total splitting Δ' and of the strength ratio η in the exciton doublet. The method which we use, already reported in a preliminary publication,[15] consists in the application of uniaxial stresses which further split the exciton, allowing a separate analysis of the positions and intensities of all components. This is done as a function of the applied perturbation in a range of stresses where nonlinear shifts due to the interaction with other energy levels are not present. With the aid of a theoretical treatment, in the limit of negligible exchange effects, we deduce the zero-stress extrapolations of both splitting and relative absorption intensities.

The experiment lends itself in a natural way to a precise determination of the deformation potentials, which are presented at the end of Sec. IV. In that section, all experimental results are reported and the method of analysis in terms of separate conduction-band valleys—i.e., differently oriented with respect to stress—is extensively described. The details of the experimental setup are given in Sec. II. This is followed by a complete theoretical analysis of the problem, which is articulated in three different parts: (i) exciton wave functions and energy levels with valence-band degeneracy and conduction-band anisotropy, but in absence of external perturbation; (ii) combined influence of the above effects and of applied uniaxial stress on the exciton levels; and (iii) calculation of absorption strengths under stress in the framework of two interfering intermediate states Γ_{15} and Δ_5, for the approximation of negligible interaction with the split-off band and other states. Finally, in Sec. V, the findings of the present research are discussed and compared with previous experimental and theoretical studies. In particular, we examine the bearance of exchange effects on the determination of the electron-mass-anisotropy splitting and the possible mechanisms to account for the non-square-root behavior observed in the high-energy tails of the TO-assisted absorption band.

TABLE I. Splitting, broadening, and intensity ratio of the exciton doublet according to different sources. Theoretical values do not include exchange effects.

Δ' (meV)	Γ (meV)	$\eta = \frac{I(\Delta_6)}{I(\Delta_7)}$	Experiment
0.29 ± 0.05	0.17 [a]	5.7 ± 0.5	Present work
0.35 ± 0.05	0.13	3	Wavelength-modulated absorption [b]
0.20 ± 0.05	<0.21	5 ± 1 [c]	Wavelength-modulated absorption [d]
0.40 ± 0.10	0.34		Luminescence [e]
		7.0 ± 1.5 [c]	λ modulation with stress [f]
Δ			Theory
0.32			Variational with SO interaction [g]
0.46			Variational without SO interaction [h]
0.30			Perturbative without SO interaction [i]
0.60			Variational without SO interaction [j]

[a] In a previous paper (Ref. 6), the total width 2Γ has been erroneously reported for Γ.
[b] Reference 7.
[c] Value inferred from the data reported in the quoted reference.
[d] Reference 8.
[e] Reference 10.
[f] Reference 27.
[g] Reference 14.
[h] Reference 11.
[i] Reference 12.
[j] Reference 21.

II. EXPERIMENTAL DETAILS

The wavelength modulation for λ-derivative optical absorption has been achieved by use of an oscillating quartz slab placed next to the exit slit inside a 1-m monochromator. Recording of the modulated intensity ΔI and total intensity I, as detected by a Si diode, allowed the measurement of

$d\alpha/d\lambda \propto (1/I)(\Delta I/\Delta\lambda)$. In order to optimize signal-to-noise ratio and resolution, the modulation amplitude $\Delta\lambda$ and the spectral slit width were kept equal,[16] and were such to result in an overall instrumental resolution of about 0.3 meV. Reduction by a factor of 2 of both slit width and modulation amplitude did not produce noticeable changes—at least within experimental error—in the line shape of the TO-phonon-assisted excitonic transition under study; this led us to assume that the observed linewidth was essentially of intrinsic origin. Experimental spectra have been analyzed following standard procedures of wavelength-modulation spectroscopy.[16,17]

The material was p-type Si, with resistivity of 21 000 Ω cm. The samples were cut into parallelepipeds, with basis ranging between 2 and 10 mm^2 and height of 15 mm, the long edge being [001] or [111] and parallel to the direction of the applied stress. All samples were x-ray oriented to $\pm 1°$. Compressional stress, ranging from zero to 1600 kg/cm^2, was applied with an apparatus similar to that described by Cuevas and Fritzsche[18]; an improvement in stress uniformity, however, was obtained by not glueing the samples in position, but rather inserting indium or lead spacers between sample and pistons. It was experimentally verified that, with this arrangement, the stress resulted uniform to better than 5%.

The entire stressing apparatus was immersed in liquid nitrogen. A gaseous overpressure of some tenths of an atmosphere was maintained over the liquid in order to prevent the formation of bubbles. It is important to emphasize that the linewidth which was observed at liquid-nitrogen temperature differed at most by 10% from the one we measured at 2 K, thus rendering experiments at liquid-helium temperature relatively unnecessary.

III. 1S EXCITON UNDER UNIAXIAL STRESS THEORY

In this section we intend to recall the mechanisms which are responsible for the splitting of the excitons in absence of any external perturbation. We will then outline the approximations which we use in calculating the energy position and intensity of the exciton peaks in presence of uniaxial stress. The results are to be used later in the analysis of the experimental results.

A. Unperturbed spectrum

The fundamental absorption edge in Si corresponds to indirect excitonic transitions between the top of the Γ_8^+ valence band and the six equivalent Δ-valley minima of the conduction band.[19] Transitions with all phonons are allowed, but we restrict ourselves to the case of TO-phonon-assisted transitions, which are by far the most intense and the only ones which can be studied with good accuracy in a stress experiment.

In the following we will not explicitly write the envelope part of the total exciton wave function. As we consider the 1S state, the envelope is not perturbed by uniaxial stress, at least in first approximation. For the holes, we use the $|J,m_J\rangle_u$ representation where u specifies the quantization axis. Taking the latter parallel to z, we have[20]

$$\begin{aligned}
&\left|\tfrac{3}{2},\tfrac{3}{2}\right\rangle_z = -(1/\sqrt{2})(x+iy)\alpha\,,\\
&\left|\tfrac{3}{2},\tfrac{1}{2}\right\rangle_z = (1/\sqrt{6})[2z\alpha-(x+iy)\beta]\,,\\
&\left|\tfrac{3}{2},-\tfrac{1}{2}\right\rangle_z = (1/\sqrt{6})[2z\beta+(x-iy)\alpha]\,,\\
&\left|\tfrac{3}{2},-\tfrac{3}{2}\right\rangle_z = (1/\sqrt{2})(x-iy)\beta\,,
\end{aligned} \tag{1}$$

where α and β are the spin functions. For the electrons, we take the quantization axis parallel to the valley direction. The electron wave function will be denoted $\delta_u\alpha$ or $\delta_u\beta$, where $u=x,y,z$. If we neglect the electron spin, which does not play a role in the calculation of the energy, we will define the four excitonic functions as follows:

$$\begin{aligned}
\phi_1^u &= \left|\tfrac{3}{2},\tfrac{3}{2}\right\rangle_u\delta_u\,,\\
\phi_2^u &= \left|\tfrac{3}{2},\tfrac{1}{2}\right\rangle_u\delta_u\,,\\
\phi_3^u &= \left|\tfrac{3}{2},-\tfrac{1}{2}\right\rangle_u\delta_u\,,\\
\phi_4^u &= \left|\tfrac{3}{2},-\tfrac{3}{2}\right\rangle_u\delta_u\,.
\end{aligned} \tag{2}$$

Of course, there exist three sets of excitons ($u=x$, y, or z) with the wave functions (2), which behave independently. In order to have a complete description of the crystal, they have to be considered additively.

If one takes into account only the band properties of the crystal, the states corresponding to the functions (2) are degenerate. However, there are two purely excitonic effects which can change this situation. The first is related to the axial character of an exciton constructed with an electron in a particular valley direction u. The symmetry properties of the exciton are those of the electron group C_{4v} (a subgroup of the hole group O_h). This effect has been considered by several authors[11,12,21,22] which take into account the electron-mass anisotropy in the electron-hole interaction. The anisotropy induces S-D interactions resulting in a shift of the 1S level towards lower energy and in a twofold splitting. (There are other S-D interactions coming from the particular form of the valence band. They produce only a shift of the levels and are of little importance to us.) It has been shown that the upper state (Δ_6 in the C_{4v} group) corresponds to the functions ϕ_2^u and ϕ_3^u, the lower state (Δ_7) to ϕ_1^u and ϕ_4^u.[23] We call Δ the splitting between Δ_7

and Δ_6. The most accurate theoretical value for Δ is, as discussed in Sec. I, ~0.3 meV.

As the S and D states are mixed, the functions ϕ_i^u are not completely correct to describe the 1S exciton. However, the mixing is weak and it can be neglected, in the present case, unless the S level comes in the vicinity of a D level under the action of the external perturbation.

The second excitonic effect to be considered is the exchange interaction which splits the excitons into singlet and triplet states. Due to the different location of the electron and the hole in k space, this effect is considerably weaker in indirect-gap than in direct-gap materials.[24] A theoretical estimate of the splittings induced by exchange interaction in Si gives values of the order of some hundredths of meV,[25] i.e., experimentally not accessible. Consequently, we shall ignore exchange effects in the present treatment. They will be reconsidered in Sec. V, when their bearing on the experimental results will be discussed.

B. Effect of uniaxial stress on the exciton energy

This problem has been examined by various authors,[26] and we will use the notation of Laude *et al.*[27] However, we have to reconsider the theory to take into account the effects simultaneously introduced by the anisotropy of the electron mass and of the applied stress. Consistently with our experimental observation, we restrict our attention to effects which are linear with stress, neglecting for instance the S-D stress-dependent interactions. This is justified *a priori* because the maximum stress-induced splitting we observe for the 1S state is of order 5 meV, i.e., rather smaller than the 1S-3D separation (~12 meV). We neglect also the interaction of the Γ_8^+ valence band and of the Δ_1 conduction bands with any other band. This is supported by the results of Laude *et al.*,[27] which indicate that interband interactions do not play a role in the range of stresses of our experiment.

As shown theoretically by Pikus and Bir[28] and by Suzuki and Hensel,[29] the Γ_8^+ valence band is shifted, by the hydrostatic part of a uniaxial stress, proportionally to a deformation potential $a=a_1+a_2$. The Γ_8^+ band is also decomposed into two subbands, whose shifts are proportional to the deformation potentials $b=b_1+2b_2$ and $d=d_1+2d_2$. The conduction-band minima are shifted by the amount[27]

$$F(\hat{u},\underline{\epsilon})=\hat{u}\{\mathcal{E}_1(\epsilon_{xx}+\epsilon_{yy}+\epsilon_{zz})\underline{1} +\mathcal{E}_2[\underline{\epsilon}-\tfrac{1}{3}(\epsilon_{xx}+\epsilon_{yy}+\epsilon_{zz})\underline{1}]\}\hat{u}\,, \tag{3}$$

where $\hat{u}$ is the unit vector in the direction u of the valley considered, $\underline{1}$ is the unit diadic, $\underline{\epsilon}$ is the strain tensor, and $\mathcal{E}_1$ and $\mathcal{E}_2$ are deformation potentials. In general, the three valleys are differently shifted by the stress.

Considering the anisotropy of the electron mass and a uniaxial stress, we can write the total Hamiltonian as a 4×4 matrix H_0^u defined for the ϕ_i^u base. In the case of the ϕ_i^z base, the quantization axis being z, we obtain

$$H_0^z=a(\epsilon_{xx}+\epsilon_{yy}+\epsilon_{zz})I+F(\hat{u},\underline{\epsilon})I+H_1^z, \tag{4}$$

where I is the unity matrix and

$$H_1^z=\begin{vmatrix} -v-\frac{1}{2}\Delta & -d(\epsilon_{zx}-i\epsilon_{yz}) & -w+id\epsilon_{xy} & 0 \\ -d(\epsilon_{zx}+i\epsilon_{yz}) & +v+\frac{1}{2}\Delta & 0 & -w+id\epsilon_{xy} \\ -w-id\epsilon_{xy} & 0 & +v+\frac{1}{2}\Delta & +d(\epsilon_{zx}-i\epsilon_{yz}) \\ 0 & -w-id\epsilon_{xy} & +d(\epsilon_{zx}+i\epsilon_{yz}) & -v-\frac{1}{2}\Delta \end{vmatrix} \tag{5}$$

Here

$$v=\tfrac{1}{2}b(2\epsilon_{zz}-\epsilon_{xx}-\epsilon_{yy}),\quad w=\tfrac{1}{2}\sqrt{3}b(\epsilon_{xx}-\epsilon_{yy})\,. \tag{6}$$

For a given stress, the resolution of the equation

$$H_0^z(\Psi)=E^z\Psi \tag{7}$$

enables one to calculate the eigenvalues E_i^z and the eigenfunctions, which can be generally written

$$\Psi_i^z=\sum_{j=1}^{4}\alpha_{ij}^z\phi_j^z\,. \tag{8}$$

For the other two valleys x and y, we define H_1^x, H_1^y by performing a cyclic permutation on the indices ij of the elastic constants ϵ_{ij} and we likewise find eigenvalues and eigenfunctions. Since there are two eigenvalues E_i^u for a given u (the stress does not lift the Kramers degeneracy), and because the matrices H_0^u in general are not equivalent, there are six excitonic levels in presence of a stress. In the limit of zero stress, they converge to the doublet Δ_6 and Δ_7.

In the above approach we used three different quantization axes (x, y, z). In this manner, the anisotropy of the electron mass gives a diagonal and identical contribution in the three matrices H_1^u, but the stress matrix elements have to be defined

for each quantization (or valley) considered. It is of course possible to work with only one quantization axis, chosen parallel to the stress. For each of the valleys it will then be necessary to calculate the matrix elements due to the mass anisotropy. Therefore, the two methods require the same extent of work.

C. Absorption intensities

The strength and the energy dependence of an allowed indirect absorption process are described by the following expression for the absorption coefficient[30]:

$$\alpha(h\nu) = C(h\nu - E_0)^{1/2}, \tag{9}$$

where C is related to the transition matrix elements and to the exciton total mass and E_0 is the energy of the minimum of the 1S excitonic branch plus the energy of the assisting phonon (emission case). For k-independent transition matrix elements and mass, C is a constant and Eq. (9) corresponds to parabolic dispersion; we shall use such approximation here because strong nonparabolicity effects, such as the mass reversal encountered in Ge,[13] should be unimportant in Si.[1,22] This point will be discussed more in detail later.

Indirect absorption just above threshold can occur via two channels. The first corresponds to an optical transition of the electron from the top of the valence band $(v_0, k=0)$ and any conduction band $(c_i, k=0)$, and by a phonon scattering to points (c_0, k) near the bottom of the conduction band at k_0. In the second process, a vertical transition between (v_i, k) and (c_0, k) and a scattering of the hole from (v_i, k) to $(v_0, 0)$ create an exciton of wave vector k. All these processes involve various bands and take place concurrently. In general, the number of intermediate states c_i and v_i which is taken into account, is *a priori* restricted—solely on the basis of energy denominator arguments—to the bands which are closest to v_0 and c_0. This enables the assumption, done by various authors,[27,31] that the only two intermediate states $(c_0, 0)$ (namely, Γ_{15}) and (v_0, k_0) (namely, Δ_5) are important in the case of TO-assisted transitions. For constant C then we have

$$C \propto \sum_t \left| \frac{\langle v_0, 0|\vec{e}\cdot\vec{p}|c_0, 0\rangle\langle c_0, 0|H^t_{ep}|c_0, k\rangle}{E(c_0, 0) - E(c_0, k_0) + \hbar\omega_0} + \frac{\langle v_0, 0|H^t_{ep}|v_0, k_0\rangle\langle v_0, k_0|\vec{e}\cdot\vec{p}|c_0, k_0\rangle}{E(v_0, 0) - E(v_0, k_0) + \hbar\omega_0} \right|^2, \tag{10}$$

where $\vec{e}$ is the polarization vector of the light, $\vec{p}$ is the electron momentum operator, and H^t_{ep} is the electron-phonon operator for the phonon branch t. In our case of TO phonons, t specifies the phonon polarization.

Quantity (10) cannot be directly calculated, mainly because the Hamiltonian H^t_{ep} is not accurately known. However, one can determine the dependence on $\vec{k}_0$, $\vec{e}$, and t of each of the matrix elements appearing in Eq. (10). This is done below and will be useful in calculating the relative strength of the transitions towards different excitonic states. The relative weight of the two processes interfering to give (10) can also be characterized, as done in Ref. 31, by two real quantities Q_T [in the case of the (v_0, k_0) intermediate state] and W_T [for the $(c_0, 0)$ intermediate state].

For the analysis of (10), the final excitonic state must be defined and the electron spin must be specified. We will use the $\phi^u_i\eta$ base ($\eta = \alpha$ or β), where the ϕ^u_i are defined by Eqs. (2). With the above choice, we can express the absorption corresponding to the final state $\phi^u_i\eta$ as proportional to $\sum_t |M^{ut}_{i\eta}|^2$, where

$$M^{ut}_{i\eta} = Q_T f^{ut}_{i\eta}(\vec{e}) + W_T g^{ut}_{i\eta}(\vec{e}). \tag{11}$$

Here $f^{ut}_{i\eta}$ and $g^{ut}_{i\eta}$ give the spatial and spin dependence of $M^{ut}_{i\eta}$. For a general solution $\Psi^u_i\eta = \sum_j \alpha_{ij}\phi^u_j\eta$, the absorption is then proportional to

$$n^u_{i\eta} = \sum_t |\alpha_{ji} M^{ut}_{i\eta}|^2. \tag{12}$$

In the present problem, the two states with wave functions $\Psi^u_i\alpha$ and $\Psi^u_i\beta$ are always Kramers degenerate and we can define the absorption intensity for the eigenvalue E^u_i and eigenfunction Ψ^u_i obtained by solving Eq. (7). It is proportional to

$$N^u_i = \sum_\eta N^u_{i\eta}. \tag{13}$$

We have calculated the quantities $M^{ut}_{i\eta}$ in the same way as done in Ref. 31, and we obtain for the z valley,

$$\begin{aligned} &M^{zx}_{1\alpha} = -M^{zx}_{4\beta} = -iM^{zy}_{1\alpha} = -iM^{zy}_{4\beta} = -(W_T/2\sqrt{2})e_z, \\ &M^{zt}_{2\alpha} = M^{zt}_{3\beta} = (1/\sqrt{6})(Q_T + W_T)e_t, \\ &M^{zx}_{3\alpha} = -M^{zx}_{2\beta} = iM^{zy}_{3\alpha} = iM^{zy}_{2\beta} = (W_T/2\sqrt{6})e_z, \\ &M^{zt}_{4\alpha} = M^{zt}_{1\beta} = 0, \end{aligned} \tag{14}$$

where $t = x$ or y.

Definitions (11)–(14) enable the calculation of the relative strengths of the components of energy E^z_i and wave function Ψ^z_i. For valleys x and y one readily calculates the quantities $M^{ut}_{i\eta}$ by a cyclic permutation of the indices x, y, z in Eqs. (14), so that all the intensities N^u_i can be determined.

The above results—which we may recall—have been obtained with the same approximations used by Smith and McGill,[31] which allow for the possibility of interference between the two transition

TABLE II. Relative intensities of the exciton components under [001] and [111] uniaxial stresses. The calculation is made in the limit of low and high stress. In the latter case, defined by the conditions γS or $|\delta S| \gg \frac{1}{2}\Delta$, a comparison between the theoretical and experimental values enables us to determine W_T, Q_T, and $R_T = W_T + Q_T$. The best-fit values we obtain $W_T = Q_T = \pm\sqrt{30}$ are used to determine the calculated values.

Stress direction	Component and light polarization		Intensity for $\gamma S \ll \frac{1}{2}\Delta$	Calc. value	Intensity for $\gamma S \gg \frac{1}{2}\Delta$	Calc. value	Expt. value
[001][a]	B_1	$\parallel$	$\frac{1}{6}W_T^2$	5	$\frac{1}{6}W_T^2$	5	4 ± 2
		$\perp$	$\frac{1}{3}R_T^2$	40	$\frac{1}{3}R_T^2$	40	45 ± 3
	B_2	$\parallel$	$\frac{1}{2}W_T^2$	15	$\frac{1}{2}W_T^2$	15	17 ± 3
		$\perp$	0	0	0	0	0
	B_3	$\parallel$	0	0	$\frac{1}{6}R_T^2$	20	15 ± 3
		$\perp$	$\frac{1}{2}W_T^2$	15	$\frac{5}{12}W_T^2+\frac{1}{12}R_T^2$	23	21 ± 3
	$B4$	$\parallel$	$\frac{2}{3}R_T^2$	80	$\frac{1}{2}R_T^2$	60	64 ± 5
		$\perp$	$\frac{1}{6}W_T^2+\frac{1}{3}R_T^2$	45	$\frac{1}{4}W_T^2+\frac{1}{4}R_T^2$	37	34 ± 3
			$\lvert\delta S\rvert \ll \frac{1}{2}\Delta$		$\lvert\delta S\rvert \gg \frac{1}{2}\Delta$		
[111][b]	A_1	$\parallel$	$\frac{1}{2}W_T^2$	15	$\frac{1}{3}W_T^2+\frac{1}{3}R_T^2+\frac{1}{3}W_TR_T$	70	69 ± 5
		$\perp$	$\frac{1}{2}W_T^2$	15	$\frac{1}{3}W_T^2+\frac{1}{3}R_T^2-\frac{1}{6}W_TR_T$	40	41 ± 3
	A_2	$\parallel$	$\frac{1}{6}W_T^2+\frac{2}{3}R_T^2$	85	$\frac{1}{3}W_T^2+\frac{1}{3}R_T^2-\frac{1}{3}W_TR_T$	30	31 ± 4
		$\perp$	$\frac{1}{6}W_T^2+\frac{2}{3}R_T^2$	85	$\frac{1}{3}W_T^2+\frac{1}{3}R_T^2+\frac{1}{6}W_TR_T$	60	59 ± 4

[a] In the calculation we use the notion that $\gamma > 0$, as deduced from the B_1-B_2 crossing for a positive stress value.
[b] In the calculation we use the notion that $\delta < 0$, as determined by Hensel and Feher (Ref. 39).

channels. Our results in the limit of zero stress do therefore become identical to theirs. This approach, however, differs from that of Laude *et al.*,[27] who consider processes that cannot interfere but act independently. This is equivalent to neglecting the products Q_TW_T appearing in the calculation (see Table II), which is not justified. On the other hand, for transitions involving one intermediate state only (i.e., W_T or $Q_T = 0$), our calculation is equivalent to that of Erlbach[32] and we have verified that identical results are obtained.

IV. EXPERIMENTAL RESULTS

A. Zero-stress spectrum

The energy derivative of the absorption coefficient over an extended range of photon energies is given in Fig. 1 for a temperature of 77 K. Four structures are observed, corresponding to transitions to the 1*S* and 2*S* exciton states, accompanied by the emission of LO and TO phonons. The relative intensity and general shape of the structures are the same as those reported earlier in the literature.[4,5]

We shall concentrate later on the TO $n = 1$ structure. However, it will appear worthwhile attempting a fit of the overall spectrum as a sum of individual contributions. Due to the extended range of energies, it is quite reasonable for the moment to neglect such fine details as the mass-anisotropy splitting. Starting from Eq. (9), we must derive an analytical expression for $d\alpha/dh\nu$ which takes into account the intrinsic and the instrumental broadening of the line. In Sec. II, we have mentioned that the latter plays a negligible role. For the former we introduce a Lorentzian broadening parameter Γ which transforms the derivative $\frac{1}{2}C(h\nu - E_0)^{-1/2}$ into[33]

$$\frac{d\alpha}{dh\nu} = \frac{C}{2}\left(\frac{h\nu - E_0 + [(h\nu - E_0)^2 + \Gamma^2]^{1/2}}{2[(h\nu - E_0)^2 + \Gamma^2]}\right)^{1/2} \qquad (15)$$

Using this law where C is a constant to fit the main TO peak of Fig. 1, we found that it decreases much too fast to account for the observed high-energy tail of the structure. At an energy 10 meV above the exciton threshold, we would require an increase of C by 70%. This fact is observed both at 4 and 77 K and is common to the spectra reported in Refs. 4 and 5. An anomalous Stark-effect behavior in the same energy region has been reported but not explained.[34] This cannot be understood by absorption processes located at lower energy (e.g., TA-assisted transitions, falling to the left of the figure). The experiment shows that

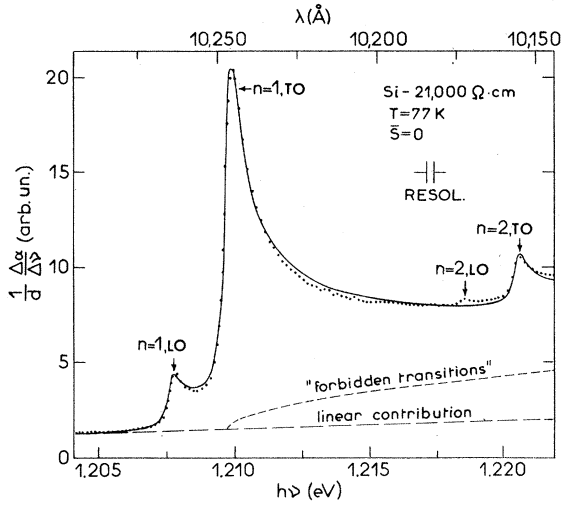

FIG. 1. Extended wavelength-modulated absorption spectrum for LO- and TO-assisted excitonic transitions showing 1S and 2S states (dots). The solid line is a best fitting calculation; this includes a linear contribution from lower-lying thresholds and a square-root term possibly related to forbidden transitions (both shown).

these give a small linear contribution in the region 1.195 to 1.207 eV, which can be safely extended to higher energies.

A good fitting of the spectrum of Fig. 1 is obtained by adding to the TO contribution of type (15), where C is a constant, a term

$$\frac{d\alpha'}{dh\nu} = \tfrac{3}{2}C'(h\nu - E_0)^{1/2}, \qquad (16)$$

where C' is also a constant. Equation (16) is characteristic of forbidden transitions and we should question the possibility of such occurrence. Selection rules for transitions are calculated along the Δ line and they restrict absorption to particular relative orientations of the valley direction and of the polarization of both the photon and transverse phonon. Out of the Δ line, the selection rules are less restrictive and new TO-assisted transitions become possible, with an energy dependence given by Eq. (16). Forbidden transitions have been observed in Ge for TA-assisted processes.[35,36] The coexistence of allowed and forbidden TO transitions has also been assumed to improve the theoretical line shape of electron-hole drop luminescence in Ge.[36] However it is very difficult to theoretically calculate the relative contribution of the allowed and forbidden transitions, and the good fit we obtain is perhaps only accidental.

The best-fitting curve is reported in Fig. 1. For transitions to the 1S state, the following terms were taken into account: (i) linear contribution from lower-energy structures not shown in the figure; (ii) LO-allowed transitions, with strength C^1_{LO} and broadening Γ^1_{LO}; (iii) TO-allowed transitions (C^1_{TO} and Γ^1_{TO}), and (iv) TO-forbidden transitions, with strength C'^1_{TO} [Eq. (16)]. We ignore possible LO-forbidden transitions and broadening of the forbidden transitions which, like the exciton splitting, give just small or localized effects. As to transitions to the $n=2$ state, we considered only allowed TO, characterized by C^2_{TO} and a Γ^2_{TO} equal to Γ^1_{TO}. The fitting parameters are

$$C^1_{LO}/C^1_{TO}=0.14, \quad C^2_{TO}/C^1_{TO}=0.15,$$
$$C'^1_{TO}/C^1_{TO}=0.023 \text{ meV}^{-1}, \quad \Gamma^1_{LO}=0.20 \text{ meV},$$
$$\Gamma^1_{TO}=\Gamma^2_{TO}=0.22 \text{ meV}.$$

An alternative way to explain the shape of the absorption may be related to the nonparabolicity of the excitonic dispersion. Existing theories[1,22] do not predict such effects but neglect the Γ_8^+-Γ_7^+ interactions. Calculations are under way to determine their importance.[37] Thus, it is actually not possible to fully understand the shape of the experimental curve. The empirical law we propose gives, however, a very good analytical description of the situation.

B. Stress in the [001] direction

As previously reported,[27,38] for stress $\vec{S}\|[001]$ the exciton is split into four levels. Their positions (peaks of the experimental $d\alpha/d\lambda$ for TO-assisted transitions, reported in Fig. 2) are shown

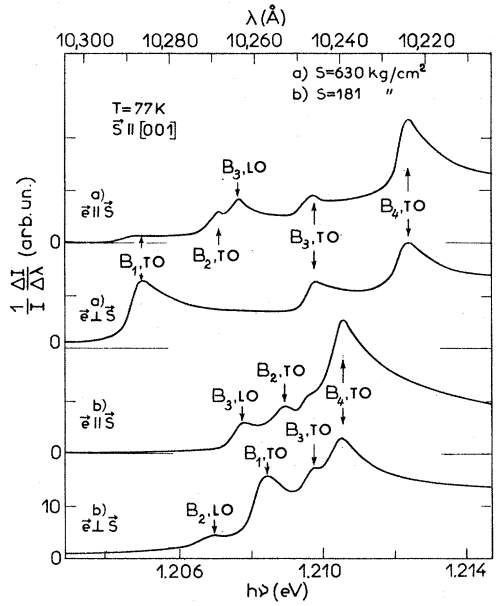

FIG. 2. TO-assisted spectra for two different values of applied [001] stress and light polarized parallel and perpendicular to it. Peaks at B_1, B_2, B_3, B_4 correspond to the fourfold splitting of the exciton discussed in Sec. IV B.

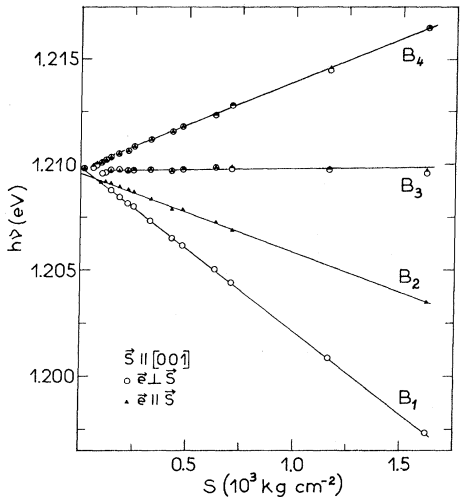

FIG. 3. Triangles and circles: energy positions of the four levels B_1–B_4 of Fig. 2, as a function of stress applied in the [001] direction. The experimental uncertainty is always less than the dot size. Straight lines: calculated from Eqs. (17) and (20) using the parameters given in Eqs. (21) and (22).

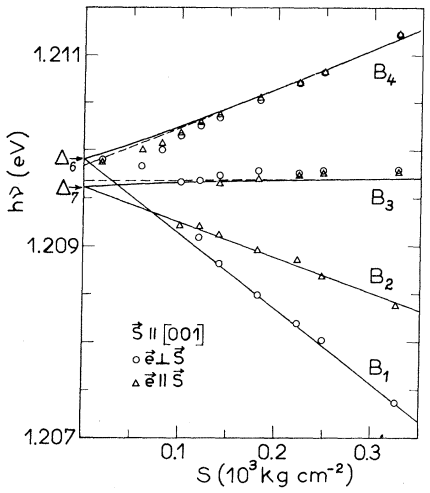

FIG. 5. Blow up of Fig. 3 in the small-stress region, showing both the general theoretical behavior of the pair B_3,B_4 from Eqs. (19), solid lines; and the linear asymptotic behavior of Eqs. (20), dashed lines. The experimental error is comparable with dot size except for B_3 where it is somewhat larger.

in Fig. 3 for light polarized perpendicular ($e_\perp$) and parallel ($e_\parallel$) to the stress. In terms of bands, the number of components is due to the twofold splitting of the valence band into the states $|\frac{3}{2}, \pm\frac{1}{2}\rangle_z$ and $|\frac{3}{2}, \pm\frac{3}{2}\rangle_z$, and to the different shift of the z-directed conduction band with respect to the equivalent x and y valleys (see scheme in Fig. 4).

The spectra of Fig. 2 differ from previously reported ones in a number of aspects: (i) we work with a resolution which enables observation of the real form of the structure; (ii) we do not have to correct the results for a dependence on $h\nu$ of the incident light intensity as in Ref. 27; and (iii) a

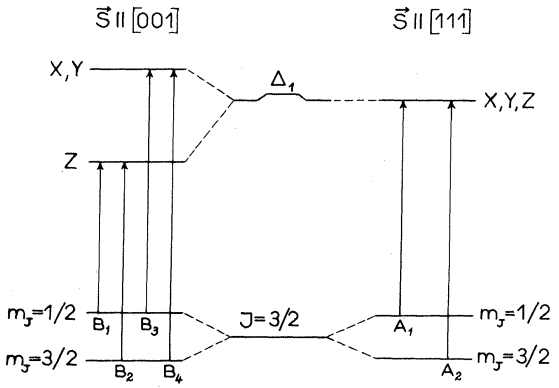

FIG. 4. Representation of the deformation-induced exciton splitting in terms of band properties, for [001] and [111] stresses. The small hydrostatic contribution is schematically shown as a shift of the conduction band.

good uniformity of the stress is achieved. This last point has been controlled by a measure of the width of the component B_1 (see Fig. 3) as a function of stress. B_1 shifts linearly and strongly with S, so that a stress nonuniformity readily induces a broadening. This criterion enables us to estimate that in our case the stress is uniform to within ±5%. Figure 5 is a blow up of Fig. 3 in the small-stress region. It is seen that the shift of the levels extends linearly down to stresses of about 150 kg/cm^2. At lower values, the peaks become partially unresolved and the experimental points do not have a precise meaning. Also, the zero-stress linear extrapolations of the various levels are different and do not converge to a doublet. This occurrence will become clear in a moment. It should be mentioned, in any case, that the precise definition of zero stress is made somewhat difficult by the occurrence of a very weak, but observable, spontaneous dichroism for $e_\parallel$ and $e_\perp$ spectra. It is not unconceivable that surface tensions may be the cause, upon cooling, of a built-in stress pattern. Due to the barlike shape of the sample, this would have an approximately axial symmetry along the sample length, and would simply add to (or substract from) the applied force. With this in mind, we have proceeded to a small zero adjustment with the criteria exposed immediately after Eq. (20).

As we have discussed in Secs. III B and III C, in general, we must separately consider the three valley directions to calculate the theoretical positions and intensities of the spectral components. For [001] stress we have only two cases: (i) val-

ley and stress parallel (z), and (ii) valley and stress at right angles (x,y).

1. z valley

The stress and the electron-mass anisotropy effects can simply be added, as they have the same axial character. Then the matrix (5) is diagonal and the wave functions (2) (with $u=z$) are the eigenfunctions of the system for all values of the stress. Using the relationships

$$\epsilon_{xx}=\epsilon_{yy}=S_{12}S\,,\quad \epsilon_{zz}=S_{11}S\,,$$
$$\epsilon_{yz}=\epsilon_{zx}=\epsilon_{xy}=0\,,$$

where S_{ij} are the elastic compliance coefficients, and S is the stress, taken positive here; thus, we calculate the following energies:

$$\begin{aligned}E(B_1)&=E_2^z=E_3^z=+\tfrac{1}{2}\Delta-(\alpha+2\beta+\gamma)S\,,\\ E(B_2)&=E_1^z=E_4^z=-\tfrac{1}{2}\Delta-(\alpha+2\beta-\gamma)S\,,\end{aligned}\tag{17}$$

where B_1 and B_2 correspond to the notations of Figs. 2–5. The experiment shows that α, β, and γ are positive. They are defined by

$$\begin{aligned}&\alpha=(a+\mathcal{E}_1)(2S_{12}+S_{11})\,,\\ &\beta=-\tfrac{1}{3}\mathcal{E}_2(S_{11}-S_{12})\,,\quad \gamma=-b(S_{11}-S_{12})\,.\end{aligned}\tag{18}$$

Relations (12)–(14) enable the calculation of the intensities $I(B_1)$ and $I(B_2)$ of B_1 and B_2. The wave functions $\{\Psi_i^z\}=\{\phi_i^z\}$ being stress independent, $I(B_1)$ and $I(B_2)$, for light polarized parallel or perpendicular to the stress, are also stress independent. The normalized theoretical expressions of $I(B_1)$ and $I(B_2)$ are reported in Table II.

2. x and y valleys

Here stress and mass anisotropy act in perpendicular directions and do not give effects which can be just added. Solving the systems $H_0^u(\Psi)=E^u\Psi$, with $u=x,y$ and H_0^u from Eqs. (4)–(6), we find

$$\begin{aligned}E(B_3)&=(-\alpha+\beta)S-\tfrac{1}{2}[3\gamma^2S^2+(\gamma S+\Delta)^2]^{1/2}\,,\\ E(B_4)&=(-\alpha+\beta)S+\tfrac{1}{2}[3\gamma^2S^2+(\gamma S+\Delta)^2]^{1/2}\,.\end{aligned}\tag{19}$$

For high stress, namely, $4\gamma^2S^2\gg\Delta^2$, Eqs. (19) can be approximated by the linear relationships

$$\begin{aligned}E(B_3)&=(-\alpha+\beta-\gamma)S-\tfrac{1}{4}\Delta\,,\\ E(B_4)&=(-\alpha+\beta+\gamma)S+\tfrac{1}{4}\Delta\,.\end{aligned}\tag{20}$$

Equations (17) and (20) for $S\to 0$ lead to the relationship $R=[E(B_1)-E(B_2)]/[E(B_1)-E(B_4)]=4$. It is this boundary condition which we have used to set the exact zero position of the stress. This procedure is acceptable even if exchange effects are not negligible, as we shall prove in Sec. V.

The B_3 (B_4) component corresponds to the wave functions ϕ_1^u, ϕ_4^u (ϕ_2^u, ϕ_3^u) for $S=0$ and to the wave functions $|\tfrac{3}{2},\pm\tfrac{1}{2}\rangle_z\delta_u$ ($|\tfrac{3}{2},\pm\tfrac{3}{2}\rangle_z\delta_u$) for stress high enough that the effects are entirely described in terms of band properties ($\gamma^2S^2\gg\tfrac{1}{4}\Delta^2$). For stresses in the intermediate range, $\gamma^2S^2\sim\tfrac{1}{4}\Delta^2$, the eigenfunctions of the system are stress dependent, as will be the strengths of B_3 and B_4. Since the general formulas of the component intensities are complicated, we give them for the two limiting cases $\gamma^2S^2\ll\tfrac{1}{4}\Delta^2$ and $\gamma^2S^2\gg\tfrac{1}{4}\Delta^2$ in Table II.

Using Eqs. (17) and (20), we have obtained an excellent fit of the experimental data (see Fig. 3, solid lines). The best-fitting parameters have been determined without taking into account the B_3 points which are considered to be insufficiently accurate. The calculated curves are also shown in the amplified plot of Fig. 5 (dashed lines), along with the nonasymptotic curves for B_3, B_4 given by Eq. (19) (solid lines). The following numerical values are found (in eV kg^{-1} cm^2):

$$\begin{aligned}&\alpha=(5.4\pm1)\times10^{-7}\,,\quad \beta=(26.0\pm1)\times10^{-7}\,,\\ &\gamma=(20.5\pm1)\times10^{-7}\,;\end{aligned}\tag{21}$$

and for the splitting

$$\Delta'=0.29\pm0.05\ \text{meV}\,,\tag{22}$$

where the prime is used to evidence its experimental origin.

Since the linewidth of the spectral components is relatively insensitive to stress, we determine the absorption strengths by a measure of the height of the various peaks of Fig. 2, which are further normalized to 100 for each light polarization. The errors are relatively important, typically ±10% on the average. As shown in Fig. 5, the components are well resolved only for $S>150$ kg/cm^2, which is what we have defined the high-stress region ($4\gamma^2S^2\gg\Delta^2$). Therefore, we are unable to observe the theoretically predicted variation of $I(B_3)$ and $I(B_4)$ which takes place at lower stress values. For stresses between 150 and 1500 kg/cm^2, we do not observe measurable strength changes.

The relative absorption intensities are reported in Table II and are compared with the theoretical expressions and the best-fit values obtained for $W_T=Q_T=\pm\sqrt{30}$. (From the analysis of the results for $\vec{S}\|[001]$ one determines only $|W_T|^2/|W_T+Q_T|^2$. The analysis of the data for $\vec{S}\|[111]$—see below—enables the determination of W_T/Q_T.) The agreement between theory and experiment is remarkably good.

At zero stress, the intensities $I(\Delta_6)$ and $I(\Delta_7)$ of the two lines of the doublet are given by

$$I(\Delta_6)=\tfrac{1}{6}W_T^2+\tfrac{2}{3}(W_T+Q_T)^2\,,\quad I(\Delta_7)=\tfrac{1}{2}W_T^2\,.\tag{23}$$

The ratio $\eta=I(\Delta_6)/I(\Delta_7)$ is then found to be $\eta=5.7$

± 0.5. This value should be compared to $\eta \simeq 7$ estimated by Smith and McGill, who use the experimental results of Laude *et al.*[27] The value found here is likely to be more accurate due to better experimental conditions (e.g., stress range giving only linear effects) and to a thorough theoretical analysis. The present data are the first ones to establish the validity of the two-intermediate-state approximation, with the due inclusion of mutual interference.[31]

C. Stress in the [111] direction

In the present case, the three conduction valleys are equivalent for the stress. As the stress and the electron-anisotropy work in different directions, their effects are not directly added. Solving Eq. (7), we find the following eigenenergies:

$$E(A_1) = -\alpha S - (\tfrac{1}{4}\Delta^2 + \delta^2 S^2)^{1/2}, \qquad E(A_2) = -\alpha S + (\tfrac{1}{4}\Delta^2 + \delta^2 S^2)^{1/2}, \tag{24}$$

where

$$\delta = \tfrac{1}{6}\sqrt{3}\, d S_{44}. \tag{25}$$

The doublet corresponds to the valence band being split into the states $|\tfrac{3}{2}, \pm\tfrac{3}{2}\rangle_{[111]}$ and $|\tfrac{3}{2}, \pm\tfrac{1}{2}\rangle_{[111]}$. In the high-stress approximation—i.e., for $4\delta^2 S^2 \gg \Delta^2$—we can approximate the energies of (24) by

$$E(A_1) \simeq -\alpha S - |\delta S|, \quad E(A_2) \simeq -\alpha S + |\delta S|. \tag{26}$$

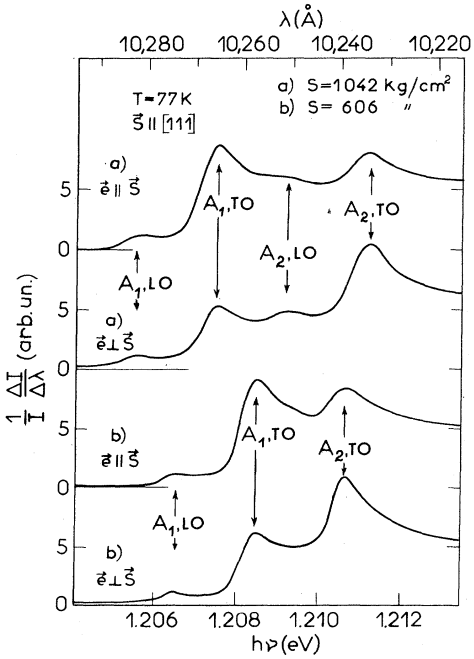

FIG. 6. Analogous to Fig. 2 except for stress parallel to the [111] direction. The A_1, A_2 lines correspond to the twofold splitting of the exciton discussed in Sec. IV C.

Experimentally, we observe two lines, as shown in Fig. 6 for the TO-assisted region. In Fig. 7 we report the energy positions of the A_1, A_2 peaks. As for [001] stress, the shifts are linear, at least in the region where the two components are resolved.

For $S \geq \Delta/2\delta$ we have fitted the experimental points with the straight dashed lines shown in Fig. 7. These lines converge, at zero stress, to points separated by $\simeq 0.04$ meV. However, as the energy precision of each experimental point is evaluated to within ± 0.05 meV, we may conclude that the experiment follows the theoretical law (26). Thus we determine the experimental values $\alpha = (3.9 \pm 1) \times 10^{-7}$ eV kg^{-1} cm^2 and $|\delta| = (17.9 \pm 1) \times 10^{-7}$ eV kg^{-1} cm^2. [The present experiment does not enable the determination of the sign of δ. However, δ is known to be negative.[39] This fact will be used for the calculation of the intensities $I(A_1)$ and $I(A_2)$.] Using for Δ the value $\Delta' = 0.29$ meV found previously, we can calculate the nonapproximated energies by use of Eq. (24). The results, shown in Fig. 7 by solid lines, are in good agreement with the experiment. The [111] data do not allow, however, an independent determination of the splitting.

The experimental intensities of the components A_1 and A_2 have been estimated as in the case of [001] stress. Here again we are able to determine the intensities only for the "high-stress" limit. The experimental values are compared with the theoretical ones, as calculated for the same W_T, Q_T values used before. The agreement is excellent, confirming the validity of the approximations used in the theory.

D. Deformation potentials

Use of Eqs. (18) and (25) allows evaluation of the deformation potentials directly from the exper-

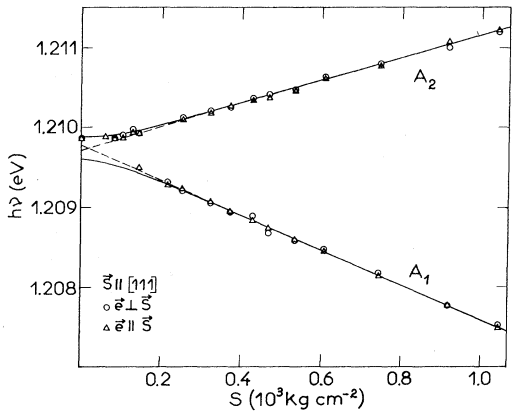

FIG. 7. Circles and triangles: plot of the A_1, A_2 line vs stress, applied along [111]. Solid lines, calculated from Eqs. (24); dashed lines, calculated from Eqs. (26). The parameters used are given in the text.

TABLE III. Deformation potentials, as obtained in the present work, compared with other available data and with theoretical calculations. The values are derived from the measured $\alpha, \beta, \gamma, \delta$ through Eqs. (18) and (25) and the use of elastic compliance coefficients S_{ij} derived from Ref. 40. The splitting anisotropy parameter B is defined in the text.

b (eV)	d (eV)	$\mathcal{E}_2$ (eV)	$(\mathcal{E}_1+a)_{[100]}$ (eV)	$(\mathcal{E}_1+a)_{[111]}$ (eV)	B	Technique
-2.14 ± 0.1	$-5.1\ \pm0.3$	-8.1 ± 0.3	1.6 ± 0.3	1.2 ± 0.3	0.87 ± 0.05	Present work
$-2.1\ \pm0.1$	-4.85 ± 0.15	-8.6 ± 0.4	2.0 ± 0.5	1.5 ± 0.3	0.85 ± 0.05	Optical with stress [a]
-2.5	-4.9	-8.3 ± 0.5	4.5	4.3	0.73 ± 0.05	Optical with stress [b]
$-2.4\ \pm0.2$	$-5.3\ \pm0.4$	-8.6 ± 0.2	4.3 ± 0.5	3.4 ± 0.5	0.82 ± 0.05	Optical with stress [c]
	-5.2	-8.5				Anisotropic phonon scattering [d]
-1.40 ± 0.15	$-3.1\ \pm0.3$				0.84 ± 0.02 (from masses) 0.82 ± 0.05 (from deformation potential)	Cyclotron resonance [e]
-1.90 ± 0.1	-4.40 ± 0.3				0.85 ± 0.05	Cyclotron resonance [f]
			1.51 ± 0.3			Piezoresistance [g]
			1.28			Optical with stress [h]
			1.48			Piezoresistance [i]
-2.3	-5.2	-8.0				Pseudopotential [j]
-2.0	-5.1	-7.5				Pseudopotential [k]
-2.5	-4.9	-9.6				Perturbative [l]

[a] Reference 27.
[b] I. P. Akimchenko and V. A. Vdovenkov, Fiz. Tverd. Tela 11, 658 (1969) [Sov. Phys.-Solid State 11, 528 (1969)].
[c] Reference 38.
[d] R. Ito, H. Kamamura, and M. Fukai, Phys. Lett. 13, 26 (1964).
[e] Reference 39.
[f] Reference 44.
[g] M. Nathan and W. Paul, Phys. Rev. 128, 38 (1962).
[h] D. Warschauer and W. Paul, J. Phys. Chem. Solids 5, 102 (1958).
[i] W. Paul and G. L. Pearson, Phys. Rev. 98, 1755 (1955).
[j] Reference 42.
[k] Reference 43.
[l] I. Goroff and L. Kleinmann, Phys. Rev. 132, 1080 (1963).

imental best-fitting parameters $\alpha, \beta, \gamma, \delta$. The elastic compliance tensor components S_{11}, S_{12}, and S_{44} have been derived from the work of McSkimin.[40] The results are reported in Table III. For comparison, the table also lists the data from previous experiments and theories.

V. DISCUSSION AND CONCLUSIONS

We shall start in this section by considering the exchange energy, which in the analysis of the results we have *a priori* neglected, in order to estimate its possible correction to the value of the exciton splitting.

For electrons in a given valley, e.g., in the z direction, we call $J_\parallel$ and $J_\perp$ the exchange energy corresponding, respectively, to excitons constructed with hole wave functions of type z or types x and y. The matrix elements are

$$H_{ij}^{\mu\nu} = \langle \phi_i^\mu \mu \,|H_{ex}|\, \phi_j^\nu \nu \rangle \ ,$$

where H_{ex} is the exchange Hamiltonian, the ϕ_i^μ are defined by Eqs. (2), and μ and ν are the spin functions. The nonzero matrix elements are the following: $H_{11}^{\alpha\alpha} = H_{44}^{\beta\beta} = \frac{3}{4}J_\perp$; $H_{33}^{\alpha\alpha} = H_{22}^{\beta\beta} = \frac{1}{4}J_\perp$; $H_{22}^{\alpha\alpha} = H_{33}^{\beta\beta} = \frac{1}{2}J_\parallel$; $H_{12}^{\alpha\beta} = H_{21}^{\beta\alpha} = H_{34}^{\alpha\beta} = H_{43}^{\beta\alpha} = \frac{1}{4}\sqrt{3}J_\perp$; $H_{23}^{\alpha\beta} = H_{32}^{\beta\alpha} = \frac{1}{2}J_\parallel$. From the above, we can proceed as in Sec. III to calculate the positions and the absorption strengths of the exciton components, with the electron spin explicitly written.

For zero stress, the Δ_6-Δ_7 splitting can be easily evaluated for any value of $J_\parallel$, but only for $J_\perp \gg \Delta$ or $\ll\Delta$. According to Ref. 25, we are in the limit $J_\perp \ll \Delta$, which leads to the energies and relative intensities reported in Fig. 8. It is seen that for Δ_6 almost all the absorption occurs at the upper component $J_\parallel + \frac{1}{2}\Delta$, so that the structure effectively appears as a doublet with separation $\Delta + J_\parallel - \frac{3}{4}J_\perp$.

In presence of [001] stress, we have done the calculation for $J_\parallel$, $J_\perp$, and Δ much smaller than $|\gamma S|$. The results are shown in Table IV. B_1 (for $\vec{e} \perp \vec{S}$) and B_2 are shifted, respectively, by $J_\parallel$ and $\frac{3}{4}J_\perp$. Then our extrapolated zero-stress positions of the experimental B_1 and B_2 correspond to the

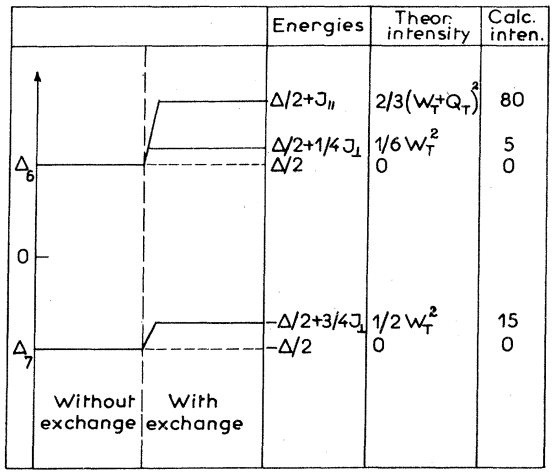

FIG. 8. Schematic representation of the effect of exchange interaction on the mass-anisotropy split exciton doublet Δ_6-Δ_7. The picture holds for $J_\perp \ll \Delta$. The dashed lines are pure triplet states. Of the two levels originating from Δ_6 the lower one is very weak. The exchange does therefore effectively widen the mass-anisotropy splitting Δ by $J_\parallel - \frac{3}{4}J_\perp$.

two most intense levels located at $\frac{1}{2}\Delta + J_\parallel$ and $-\frac{1}{2}\Delta + \frac{3}{4}J_\perp$ for $S=0$. The splitting deduced from the $B_1 - B_2$ pair is then equal to

$$\Delta' = E_{12} = \Delta + J_\parallel - \tfrac{3}{4}J_\perp . \tag{27}$$

The B_3 line is hard to analyze, while B_4 is essentially shifted by exchange to a position $\frac{3}{4}J_\parallel$ higher, so that its separation from B_1 extrapolated at $S=0$ becomes

$$E_{14} = \tfrac{1}{4}\Delta + \tfrac{1}{4}J_\parallel . \tag{28}$$

We now use the relation $J_\parallel = 3J_\perp$ found in Ref. 25 and consider the ratio

$$R = E_{12}/E_{14} = 4[1 + \tfrac{3}{4}(J_\parallel/\Delta)]/(1 + J_\parallel/\Delta) ;$$

this is a slowly decreasing function of $J_\parallel$, taking the value 4 in absence of exchange, but still 3.5 for $J_\parallel = \Delta$. This process enables us to prove that the method of setting the zero-stress position for $R=4$, as discussed after Eq. (20), is quite correct also for large exchange energy (a zero readjustment on the basis of $R=3.5$ would not be perceptible on the scale of Fig. 5). Therefore, the splitting value given in Eq. (22) is fully reliable, even though it corresponds to the overall splitting of the exciton, i.e., to Eq. (27). There are no means of telling, after the experiment, what are the relative proportions of $J_\parallel$, $J_\perp$, and Δ.

In the case $\vec{S} \parallel [111]$ the exchange effects have been calculated for $J_\parallel = 3J_\perp$ and $J_\parallel$, $\Delta \ll |\delta S|$. The results are summarized in Table V. Here the centers of gravity of A_1 and A_2, in both polarizations, are shifted by almost identical amounts. Thus the A_1-A_2 splitting is practically unaffected by exchange and once again the experiment does not allow discrimination. However, it is worth noting that the zero-stress intercepts of the dashed lines of Fig. 7 compared with the exciton energy observed in the unperturbed case can be explained only for $J_\parallel - \frac{3}{4}J_\perp \leq 0.15$ meV.

The above results are summarized as follows. The exchange interaction does not introduce further levels of appreciable strength; the zero-stress excitonic spectrum is therefore mainly associated with a doublet, whose splitting $\Delta' = 0.29 \pm 0.05$ meV

TABLE IV. Energy position and relative intensities of the exciton components for stress along [001], when exchange interaction is taken into account. $E(B_1)$ and $E(B_2)$ are the energy values given by Eqs. (17); $E(B_3)$ and $E(B_4)$ are those given by Eqs. (20), valid for $4\gamma^2 S^2 \gg \Delta^2$. The calculation is made in the limit $J_\perp$, $J_\parallel$, and $\Delta \ll |\gamma S|$. The calculated values are obtained using $W_T = Q_T = \pm\sqrt{30}$.

	Energy \ Intensity	$\vec{e} \parallel \vec{S}$ Theor.	$\vec{e} \parallel \vec{S}$ Calc.	$\vec{e} \perp \vec{S}$ Theor.	$\vec{e} \perp \vec{S}$ Calc.
	$E(B_1) + J_\parallel$	0	0	$\frac{1}{3}(Q_T + W_T)^2$	40
(B_1)	$E(B_1) + \frac{1}{4}J_\perp$	$\frac{1}{6}W_T^2$	5	0	0
	$E(B_1)$	0	0	0	0
(B_2)	$E(B_2) + \frac{3}{4}J_\perp$	$\frac{1}{2}W_T^2$	15	0	0
	$E(B_2)$	0	0	0	0
	$E(B_3) + J_\perp$	0	0	$\frac{1}{3}W_T^2$	10
(B_3)	$E(B_3) + \frac{1}{4}J_\parallel$	$\frac{1}{6}\lvert W_T + Q_T\rvert^2$	20	$\frac{1}{12}\lvert W_T + Q_T\rvert^2$	10
	$E(B_3) + \frac{1}{4}J_\perp$	0	0	$\frac{1}{12}W_T^2$	2.5
	$E(B_3)$	0	0	0	0
	$E(B_4) + \frac{3}{4}J_\parallel$	$\frac{1}{2}\lvert W_T + Q_T\rvert^2$	60	$\frac{1}{4}\lvert W_T + Q_T\rvert^2$	30
(B_4)	$E(B_4) + \frac{3}{4}J_\perp$	0	0	$\frac{1}{4}W_T^2$	7.5
	$E(B_4)$	0	0	0	0

TABLE V. Energy positions and intensities of the exciton components for stress along [111], when exchange interaction is taken into account. The energies $E(A_1)$ and $E(A_2)$ are given by Eqs. (26), where $4\delta^2 S^2 \gg \Delta^2$. The calculation is made for $J_{\parallel} = 3J_{\perp}$ and is valid in the limit $J_{\parallel}$ and $\Delta \ll |\delta S|$. Calculated values are obtained using $W_T = Q_T = \pm\sqrt{30}$.

	Energy \ Intensity	$\vec{e} \parallel \vec{S}$ Theor.	Calc.	$\vec{e} \perp \vec{S}$ Theor.	Calc.
	$E(A_1)$	0	0	0	0
(A_1)	$E(A_1)+\frac{3}{12}J_{\perp}$	$\frac{1}{12}W_T^2$	2.5	$\frac{1}{12}W_T^2$	2.5
	$E(A_1)+\frac{5}{12}J_{\perp}$	$\frac{2}{81}(2W_T - R_T)^2$	0	$\frac{2}{81}(4W_T^2 + R_T^2 + 2W_T R_T)$	9
	$E(A_1)+\frac{22}{12}J_{\perp}$	$\frac{1}{324}(49W_T^2 + 100R_T^2 + 140W_T R_T)$	67.5	$\frac{1}{324}(49W_T^2 + 100R_T^2 - 70W_T R_T)$	28.5
	$E(A_2)$	0	0	0	0
(A_2)	$E(A_2)+\frac{9}{12}J_{\perp}$	$\frac{1}{4}W_T^2$	7.5	$\frac{1}{4}W_T^2$	7.5
	$E(A_2)+\frac{21}{12}J_{\perp}$	$\frac{1}{12}(W_T - 2R_T)$	22.5	$\frac{1}{12}(W_T^2 + R_T^2 + 2W_T R_T)$	52.5

is given in Eq. (27), i.e., contains a term from exchange. Experimentally, we can only set an upper limit to such contribution of about 0.15 meV. Theoretical calculations[25] give $J_{\parallel} = 3J_{\perp} = 0.08$ meV; this yields

$$J_{\parallel} - \tfrac{3}{4}J_{\perp} = 0.06 \text{ meV}, \quad \text{hence } \Delta = 0.23 \pm 0.05 \text{ meV}.$$

More recently, by taking into account the wave-vector and frequency dependence of the dielectric function, Kane[41] has found $J_{\parallel} \simeq 3J_{\perp} = 0.16$ meV, giving $J_{\parallel} - \frac{3}{4}J_{\perp} = 0.12$ meV, which is again compatible with our upper limit. With these figures, the mass-anisotropy splitting would further reduce to only 0.17 ± 0.05 meV.

Our measured splitting is reported in Table I for comparison with other experimental results and with theories. Different aspects of this table have already been discussed in the Introduction. We shall here stress that all experimental data are inclusive of the exchange term, while theoretical figures are not. Contrary to the above estimates of $J_{\parallel}$, $J_{\perp}$, one would be tempted to say that the agreement with the theoretical value of 0.32 meV,[14] which is the best available as it takes into account coupling with the split-off valence band, is suggestive of negligible exchange effects. In Table I we also compare our experimental intensity ratio η in the doublet, Eq. (23), with previous results. Our value has the merit of having been obtained by direct observation of stress-split structures and independently of the value of Δ'. As the various lines appear fully separated only for stress large enough, it has been necessary to derive a theoretical expression for the relative strengths of the exciton components in presence of stress, in order to obtain the unperturbed η value by extrapolation. Table II shows that the calculated line intensities in the limit of "high" stress are in remarkable agreement with experiment, thus justifying our procedure. This, on the other hand, establishes the validity of a mechanism of indirect transitions via two interfering intermediate states Δ_5 and Γ_{15}.

At zero stress we report an anomalous high-energy tail of the 1S exciton absorption. This anomaly is analytically well described by assuming the existence of forbidden-TO-assisted transitions. Their strength, however, would seem exceedingly important. The anomaly can also be tentatively ascribed to the nonparabolic dispersion of the exciton. This assumption being in contradiction with existing but incomplete theories,[1,22] new developments including interband interactions[37] are needed.

The last item to be recalled is Table III, listing the deformation potential values obtained here for comparison with other sources. Our data fall somewhere in between the pseudopotential results of Saravia[42] and those of Melz,[43] and are also in good agreement with all other experiments except the early cyclotron resonance results by Hensel and Feher.[39] Very recent measurements at higher frequencies[44] come much closer to our results, especially in terms of the splitting anisotropy parameter $B = (d/\sqrt{3}b)[\frac{1}{2}S_{44}/(S_{11} - S_{12})]$, which is less critically dependent on the exact knowledge of the absolute scale of applied stress and which has been earlier determinated with the highest accuracy directly from the values of the cyclotron masses.[39]

ACKNOWLEDGMENTS

The authors are indebted to R. Generosi, R. Moretto, and S. Rinaldi for technical assitance. They have greatly benefited from stimulating dis-

cussions and correspondence with M. Altarelli, A. Baldereschi, F. I. Blount, J. C. Hensel, E. O. Kane, N. O. Lipari, and T. C. McGill. One of us (J.C.M.) is grateful to Professor F. Bassani and G. Chiarotti for their hospitality during this work and wishes to thank the CNR for financial support. This work was done as part of a CNA-CNRS collaboration between the Gruppo semiconduttori e Proprietà Ottiche dei Solidi, Rome, and the Laboratoire de Spectroscopie et d'Optique du Corps Solide (L.A. 232 du CNRS). Work by one of us (A.F.) was performed partly during a stay at the Laboratoire de Physique Appliquée, EPF-Lausanne, Switzerland.

---

*Permanent address: Laboratoire de Spectroscopie et d'Optique du Corps Solide (L.A. 232 du CNRS), 5 rue de l'Universite, Strasbourg, France.

[1]See, for instance, M. Altarelli and N. O. Lipari, *Proceedings of the Thirteenth International Conference on the Physics of Semiconductors, Rome, 1976* (North-Holland, Amsterdam, 1976), p. 811.

[2]M. Altarelli, R. A. Sabatini, and N. O. Lipari (unpublished).

[3]M. Capizzi, F. Evangelisti, P. Fiorini, A. Frova, and F. Patella, Solid State Commun. 24, 801 (1977).

[4]K. L. Shaklee and R. E. Nahory, Phys. Rev. Lett. 24, 942 (1970).

[5]T. Nishino, M. Takeda, and Y. Hamakawa, Solid State Commun. 12, 1137 (1973); 14, 627 (1974).

[6]M. Capizzi, F. Evangelisti, A. Frova, and P. Valfré, in Ref. 1, p. 857.

[7]I. Balslev, Solid State Commun. 23, 205 (1977).

[8]M. L. W. Thewalt and R. R. Parsons, Solid State Commun. 20, 97 (1976).

[9]R. B. Hammond, D. L. Smith, and T. C. McGill, Phys. Rev. Lett. 35, 1535 (1975).

[10]D. L. Smith, R. B. Hammond, M. Chen, S. A. Lyon, and T. C. McGill, in Ref. 1, p. 1077.

[11]N. O. Lipari and M. Altarelli, Phys. Rev. B 15, 4883 (1977).

[12]N. O. Lipari and A. Baldereschi, Phys. Rev. B 3, 2497 (1971).

[13]A. Frova, G. A. Thomas, R. E. Miller, and E. O. Kane, Phys. Rev. Lett. 34, 1572 (1975).

[14]N. O. Lipari and M. Altarelli (private communication).

[15]M. Capizzi, J. C. Merle, P. Fiorini, and A. Frova, Solid State Commun. 24, 451 (1977).

[16]M. Cardona, *Solid State Physics*, Suppl. 11, edited by F. Seitz, D. Turnbull, and H. Ehrenreich (Academic, New York and London, 1969).

[17]K. L. Shaklee and J. E. Rowe, Appl. Opt. 9, 627 (1970).

[18]M. Cuevas and H. Fritzsche, Phys. Rev. 137, A1847 (1965).

[19]G. G. Macfarlane, T. P. McLean, J. E. Quarrington, and V. Roberts, Phys. Rev. 111, 1245 (1958).

[20]E. O. Kane, in *Semiconductors and Semimetals*, edited by K. Willardson and A. Beer (Academic, New York, 1966), Vol. 1, p. 75.

[21]T. P. McLean and R. Loudon, J. Phys. Chem. Solids 13, 1 (1960).

[22]E. O. Kane, Phys. Rev. B 11, 3850 (1975).

[23]The Δ_6, Δ_7 notations are used in the same order as in Ref. 11, i.e., opposite to earlier papers in the literature.

[24]Y. Abe, J. Phys. Soc. Jpn. 19, 818 (1964).

[25]E. O. Kane and C. Morgan (unpublished calculation).

[26]G. L. Bir and G. E. Pikus, *Symmetry and Strain-Induced Effects in Semiconductors* (Wiley, New York, 1974).

[27]L. D. Laude, F. H. Pollack, and M. Cardona, Phys. Rev. B 3, 2623 (1971).

[28]G. E. Pikus and G. L. Bir, Fiz. Tverd. Tela 1, 1642 (1960) [Sov. Phys.-Solid State 1, 1502 (1960)].

[29]K. Suzuki and J. C. Hensel, Phys. Rev. B 9, 4184 (1974).

[30]R. J. Elliott, Phys. Rev. 108, 1384 (1957).

[31]D. L. Smith and T. C. McGill, Phys. Rev. B 14, 2448 (1976).

[32]E. Erlbach, Phys. Rev. 150, 767 (1966).

[33]B. Batz, Ph. D. thesis (Université Libre de Bruxelles, 1967) (unpublished).

[34]F. Evangelisti, A. Frova, M. Zanini, and E. O. Kane, Solid State Commun. 11, 611 (1972).

[35]C. Benoit a la Guillaume and M. Voos, Phys. Rev. B 7, 1723 (1973).

[36]R. W. Martin, Solid State Commun. 19, 373 (1976).

[37]N. O. Lipari (private communication).

[38]I. Balslev, Phys. Rev. 143, 636 (1966).

[39]J. C. Hensel and G. Feher, Phys. Rev. 129, 1041 (1963).

[40]H. J. McSkimin, J. Appl. Phys. 24, 988 (1953).

[41]E. O. Kane (private communication).

[42]L. R. Saravia, J. Phys. Chem. Solids 35, 1469 (1974).

[43]P. J. Melz, J. Phys. Chem. Solids 32, 209 (1971).

[44]J. C. Hensel and K. Suzuki (unpublished).